TÜBİTAK

Turkish Journal of Physics

http://journals.tubitak.gov.tr/physics/

Research Article

Turk J Phys
(2019) 43: 563 – 575

doi:10.3906/fiz-1907-23

Tuning the electrical and morphological characteristics of PEDOT:PSS films through mixed cosolvent addition and performance of their polymer solar cells

Çisem KIRBIYIK*
Department of Chemical Engineering, Faculty of Engineering and Natural Sciences,
Konya Technical University, Konya, Turkey

Received: 25.07.2019 • **Accepted/Published Online:** 10.09.2019 • **Final Version:** 05.12.2019

Abstract: This work aimed to reveal the influence of premixed cosolvent addition to low conductive PEDOT:PSS solution and how the optimized thin film conductivity develops. PEDOT:PSS thin films were obtained by addition of EG and MeOH cosolvent mixture (8, 10, and 15 v/v.%) and the morphological, electrical, optical, and bandgap properties of the films obtained were characterized by different techniques. The addition of mixed cosolvent can effectively control the grain size distribution and thus the conductivity. The optical characterization results revealed that the bandgap decreased with increasing volume of mixed cosolvent. The conductivity characteristics showed that the addition of 10% v/v.% EG-MeOH blend to low conductive PEDOT:PSS solution is optimal. Polymer solar cells (PSCs) were produced with a configuration of ITO/PEDOT:PSS/P3HT:PCBM/Al, which is one of the most common configurations examined. The highest efficiency of 2.7% was achieved, which resulted in a 20% enhancement (2.2%) compared to the control device.

Key words: PEDOT:PSS, polymer solar cells, electrical conductivity

1. Introduction

Polymer solar cells (PSCs) have been attracting extensive research interest since they present the unique advantages of flexibility and light weight and potential in terms of inexpensive cost and large-area fabrication [1]. PSCs commonly consist of bulk heterojunction (BHJ) architecture based on a photoactive blend of electron donor and acceptor materials between two electrodes [2,3]. Polymer:fullerene blends mostly dominate the field of high performance BHJ configuration. To the best of our knowledge, the power conversion efficiency (PCE) of BHJ-PSCs has recently exceeded 14% [4–6], which is a great improvement for applications of commercial roof-top photovoltaic systems. Despite the tremendous development in photovoltaic characteristics, BHJ solar cells have some limitations such as low charge mobility and insufficient light absorption [7]. To overcome these limitations, different techniques and approaches have been taken into consideration. In particular, the introduction of innovative materials, optimization of device architecture, and interface modifications have been reported as effective approaches to enhance the photovoltaic characteristics of PSCs [8–11].

In organic electronics, PEDOT:PSS (poly(3,4-ethylene dioxythiophene):poly(styrene sulfonate)) is one of the most commonly used conducting polymers, mainly because of its high optical transparency and solution processability [12,13]. Solution-processed photovoltaic devices have attracted significant attention owing to their ease of manufacturing and low-cost production in large-scale applications [14]. Spin coating is the

*Correspondence: ckirbiyik@ktun.edu.tr

simplest solution process for low-cost and uniform deposition of semiconductor thin films on a substrate [15]. Another advantage of this deposition technique is the easy control of thin film properties by changing solution concentration, spin speed, acceleration rate, and so on.

The PEDOT:PSS solution used in electronic devices is classified into two types: highly conductive PEDOT:PSS and low conductive PEDOT:PSS. Low conductive PEDOT:PSS has been extensively studied as a hole transport material for PSCs. In the conventional configuration, the BHJ layer is mostly located between ITO substrate coated with PEDOT:PSS film and a metal low work function electrode. However, many studies have reported that the relatively low conductivity of PEDOT:PSS is still an obstacle in optoelectronic devices due to the presence of insulating PSS [16,17]. There have been several investigations to improve the morphology, conductivity, and structure of PEDOT:PSS. According to the studies, solution treatment of PEDOT:PSS thin film or solvent addition into its solution form plays a critical role in changing the morphological or electrical properties [18]. The addition of organic solvents like ethylene glycol (EG) or dimethyl sulfoxide (DMSO) and polar organic solvents like methanol (MeOH) or isopropyl alcohol to the solution form of PEDOT:PSS results in an improvement in the electrical conductivity of the thin film obtained [19–21]. Solvent addition has been reported to initiate the macroscopic phase separation of PSS [22]. Based on a theory, the addition of a solvent with high boiling point to PEDOT:PSS solution leads to reorientation of polymer chains, developing percolating networks of high conductivity at high temperatures [18]. Together with the importance of solvent choice, the addition of two different solvents has also been reported to improve the electrical properties of PEDOT:PSS [23]. The reports have ascribed the performance enhancement to the morphological change in the PEDOT:PSS layer and the solvent-induced conductivity improvement [24]. Therefore, in the present study, the effect of mixed cosolvent of EG and MeOH was investigated on the structural changes in PEDOT:PSS, thereby effecting an improvement in the electrical properties of thin films obtained. Herein, this study show that the doping of mixed cosolvent of EG and MeOH into low conductive PEDOT:PSS solution can control the grains of PEDOT:PSS thin films obtained to improve their conductivity. The morphological and electrical properties of PEDOT:PSS thin films were characterized as a function of mixed cosolvent concentration in the range from 8% to 15% and the optimal doping concentration was found. According to the morphological analysis, the surface characteristics showed that mixture cosolvent addition can finely control the nanomorphology of PEDOT:PSS thin films. The results showed that the electrical conductivity changes from 0.0158 to 0.113 S cm^{-1} by variation in the doping concentration. Additionally, the influence of mixed cosolvent in PEDOT:PSS to enhance the PCE of BHJ polymer solar cells was investigated. Compared with the nondoped device (produced a PCE of ~2.3%), the proposed doping of mixed cosolvent of EG and MeOH approach produced a 20% enhancement in PCEs (~2.7%). The mixed cosolvent addition provides a simple way to convert the PEDOT:PSS film to its more higher conducting form and the films obtained can be used to enhance the photovoltaic characteristics of PSCs and the performance of organic electronic devices.

2. Experimental

2.1. Materials and device fabrication

Pieces of indium tin oxide-coated glass (ITO glass) with dimensions of 1.5 cm ×1.5 cm were sonicated in Hellmanex detergent solution, deionized (DI) water, acetone, isopropyl alcohol, and again DI water for 20 min successively. Then the clean ITO substrates were dried with a nitrogen gun and treated with oxygen plasma for 5 min.

Aqueous solution of PEDOT:PSS (PVP AI 4083) was acquired from Heraeus Clevios. Ethylene glycol (EG, 99.9% purity, Sigma-Aldrich) and methanol (MeOH, anhydrous, 99.8%, Sigma-Aldrich) were used without any further purification. The stock solvent doping was prepared by mixing of 50 vol.% of EG and 50 vol.% of MeOH followed by stirring for 2 h. Then 8, 10, and 15 vol.% of this premixed solvent doping were added to PEDOT:PSS aqueous solution. The resulting mixtures were stirred for 24 h, after which they were filtered using a polytetrafluoroethylene (PTFE, 0.22 µm) syringe filter. The fabrication of devices was performed in ambient atmosphere. The PEDOT:PSS thin films (50 nm) were deposited on ITO glass by spin coating at 1000 rpm for 1 min. The spin-coated surfaces were then annealed on a hot plate at 160 °C for 10 min to remove the residual solvents. Poly(3-hexylthiophene) (P3HT, Sigma-Aldrich) and (6,6)-phenyl-C61-butyric acid methyl ester (PCBM, Lumtec) were used to prepare the active layer. P3HT and PCBM (1.0:0.6 wt.% ratio) were dissolved in chlorobenzene for preparing a 40 mg/mL solution concentration. The P3HT:PCBM blend with good sealing was stirred at 70 °C for 8 h. After filtering by a PTFE filter, the active layer (150 nm) was spin coated on the PEDOT:PSS-coated substrate by spin coating at 2000 rpm for 1 min and annealed at 100 °C for 20 min. Finally, as a counter electrode, 100 nm of aluminum film was thermally evaporated on top of the P3HT:PCBM layer. The active area was 0.08 cm^2. A schematic illustration of the mixed cosolvent addition procedure and the energy level diagram of the PSCs are shown in Schemes 1a and 2b, respectively.

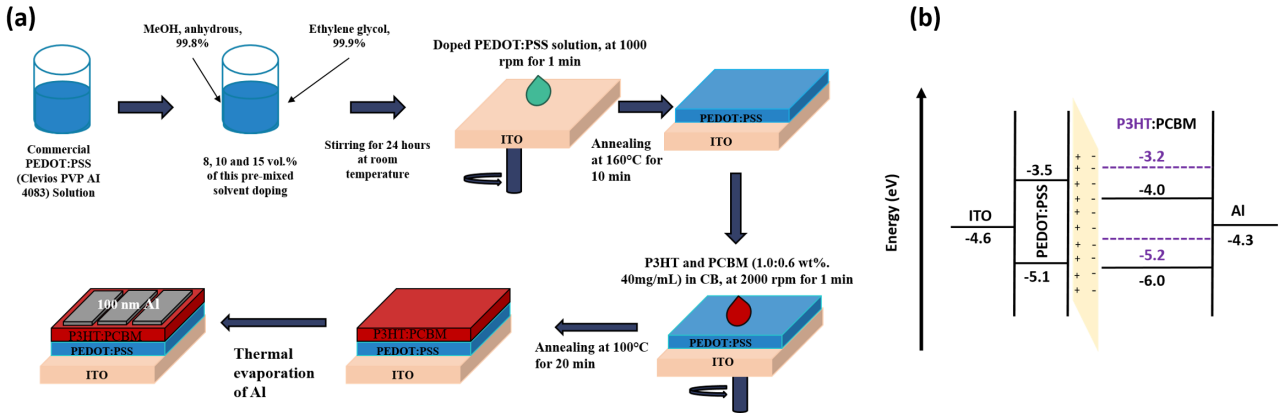

Schema (a) Schematic illustration of the mixed cosolvent addition procedure (b) and the energy level diagram of the PSCs.

2.2. Characterization

The current–voltage (J-V) measurements were performed by a solar simulator (glove-box integrated ATLAS) with an AM1.5 light source under N_2 atmosphere. The J-V curves of the PSCs produced were recorded by a Keithley 2400 source meter. Surface morphologies of the thin films were analyzed using atomic force microscopy (AFM, NT-MDT INTEGRA Solaris) in tapping mode. The conductivity analyses of the PEDOT:PSS films were conducted by 4-point probe instrument (ENTEK Elk. FPP 460 with Pt probes). The optical performance (transmittance and absorbance) was characterized by AvaSpec-ULS2048L StarLine Versatile Fiber-optic Spectrometer. The external quantum efficiencies (EQEs) were recorded as a function of wavelength from 300 nm to 800 nm using a 300 W xenon light source. The film thickness was measured with a contact profilometer (NanoMap-500LS 3D Stylus).

3. Results and discussion

For the investigation of possible alterations in the film morphologies of PEDOT:PSS surfaces doped with mixed cosolvent and for better understanding the relation between conductivity and morphology, nondoped and doped PEDOT:PSS surfaces were investigated by AFM technique. Figures 1 and 2 show representative 2D and 3D AFM images of PEDOT:PSS thin films, respectively. Quite smooth surface characteristics were observed from all PEDOT:PSS surfaces and there was no significant aggregation. The number of chain-like nanostructures (marked by circles in Figure 1a) at the surface obviously decreased after mixed cosolvent doping. In particular, these chain-like nanostructures were obscured after the addition of 10 and 15 v/v.% mixed cosolvent in Figures 1c and 1d. It could be attributed to the formation of homogeneous and closely packed PEDOT nanostructures. The AFM height images of PEDOT:PSS films are given in Figure 2. It can be seen that the roughness slightly increases after the doping of mixed cosolvent into PEDOT:PSS solution. Additionally, the average roughness (R_a) values of the corresponding films are given in Figure 3a. The average roughness (R_a) of the nondoped PEDOT:PSS film (2.55 nm) shows a result similar to that (2.64 nm) of 8 v/v.% mixed cosolvent doped PEDOT:PSS film. Moreover, 10 and 15 v/v.% mixed cosolvent-added PEDOT:PSS films were much rougher than the other films, showing R_a of 3.1 and 3.2 nm, respectively. This increasing roughness could be explained by the enhanced structural order of PEDOT:PSS [25]. The grain size distribution of the PEDOT:PSS films was determined by analysis of AFM images (5 µm ×5 µm) through the software supplied with the instrument and the results are presented in Figure 3b. The statistical grain size distribution of the PEDOT:PSS surfaces increased from 12.2 nm to 20.0 nm after the doping of mixed cosolvent. This indicates that PEDOT chains become more aggregated. As is known, PEDOT nanostructures have a direct effect on film conductivity. An increased grain size leads to a decrease in energy barriers, resulting in a conductivity improvement [26]. PEDOT chains with a linear nanostructure and larger grain size are considered to be the significant characteristic in the overall conductivity of PEDOT:PSS surfaces, since this can promote charge hopping.

The conductivity of PEDOT:PSS film is the most important parameter for high-performance PSCs and the improvement of film conductivity by doping of cosolvents has been widely investigated by researchers [27]. Figure 4 shows the conductivities of PEDOT:PSS films doped with various volumes of mixed cosolvent. As seen, the conductivity of doped films dramatically increased with the increasing mixed cosolvent volume and gave the highest conductivity of 0.113 S cm^{-1} at the doping of 10 v/v.% mixed cosolvent. Evidently, a minimum volume of 8% mixed cosolvent is required to increase the conductivity.

The mechanism for performance improvement through mixed cosolvent addition was investigated via different physical and chemical characterizations. The UV-Vis absorption and the transmittance spectra of the PEDOT:PSS films on ITO substrates are given in Figures 5a and 5b, respectively. The UV-Vis absorption spectra of all PEDOT:PSS films showed similar peaks in the wavelength range of 350–800 nm and the absorption increased for visible and near infrared (NIR) regions, starting from approximately 400 nm. It could be ascribing to the bipolaron subbandgap transition, which is a result of PSS doping in PEDOT [28]. The strongest bipolaron absorption is seen for the nondoped PEDOT:PSS surface and in the general trend absorption decreases with increasing volume of mixed cosolvent. The findings are consistent with the conductivity results. It can be seen that the transmittance increased after the addition of mixed cosolvent with the exception of the doping volume of 8%. In general, the transmittance is above 80% in the wavelength from 300 to 800 nm and the transmittance of the PEDOT:PSS film doped with 15 v/v.% mixed cosolvent is nearly 100% at 470 nm. To understand the influence of the presence of both cosolvent in PEDOT:PSS, the optical bandgaps of PEDOT:PSS films were calculated from the UV-Vis absorption data by using a Tauc plot ($(\alpha h\nu)^2$ vs. $(h\nu)$) model, where $h\nu$ is the

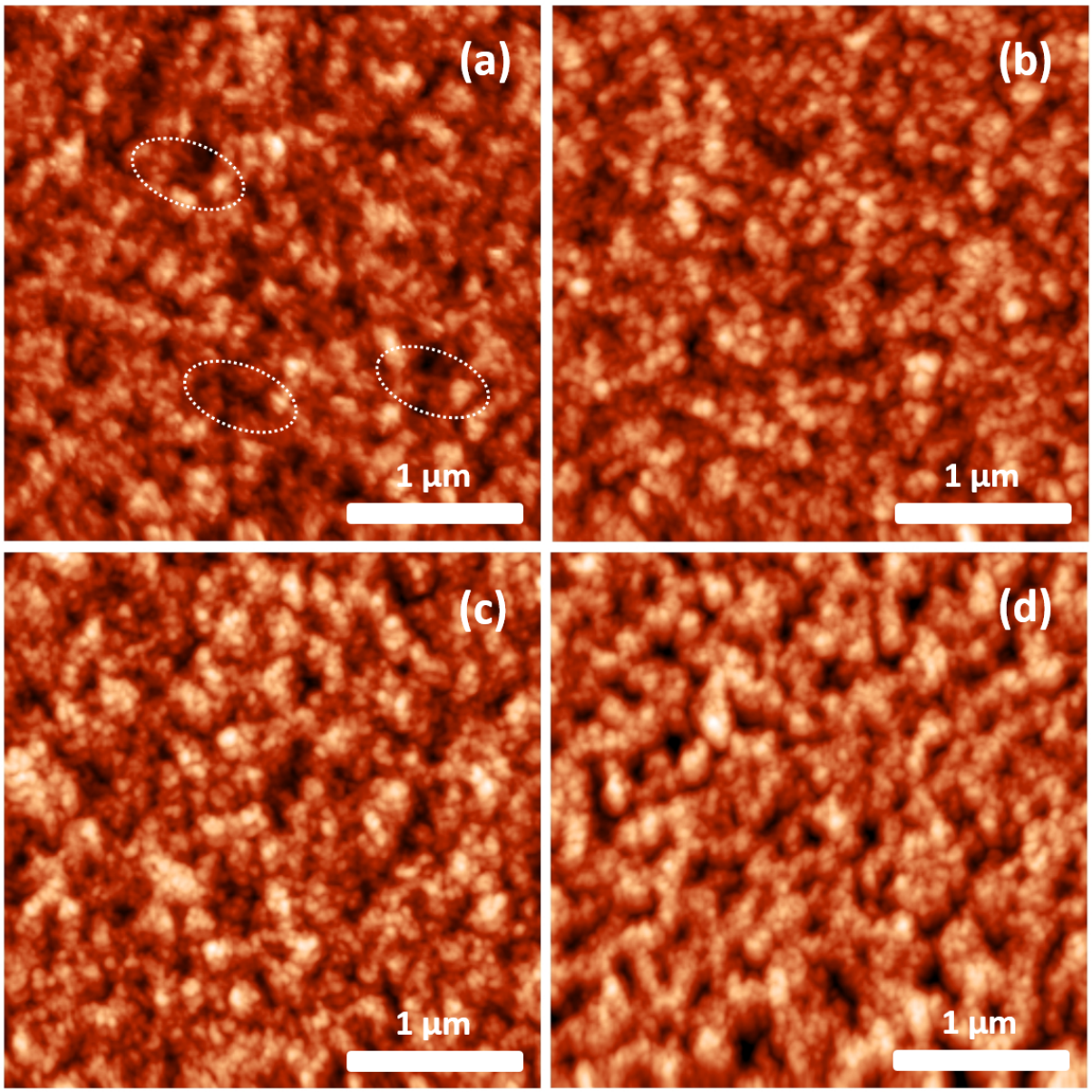

Figure 1. Representative 2D AFM images of PEDOT:PSS films (a) nondoped and doped with (b) 8 v/v.%, (c) 10 v/v.%, and (d) 15 v/v.% of mixed cosolvents of EG and MeOH.

photon energy and α is the absorption coefficient (Figure 6). The bandgap of the nondoped PEDOT:PSS was 2.22 eV, whereas it was 2.21, 2.20, and 1.98 eV with the doping of 8, 10, and 15 v/v.% mixed cosolvent, respectively. As seen, bandgap values decrease with increasing volume of mixed cosolvent. Since the conductivity is directly related to the bandgap, it could be said that the conductivity is increased by the decrease in the bandgap of PEDOT:PSS films [29]. In addition, the decrease in the bandgap after the doping procedure could be attributed to increased absorption, thereby increasing the photocurrent of the solar cell [30]. It is clear that the electrical and optical properties can simply be tuned by cosolvent addition.

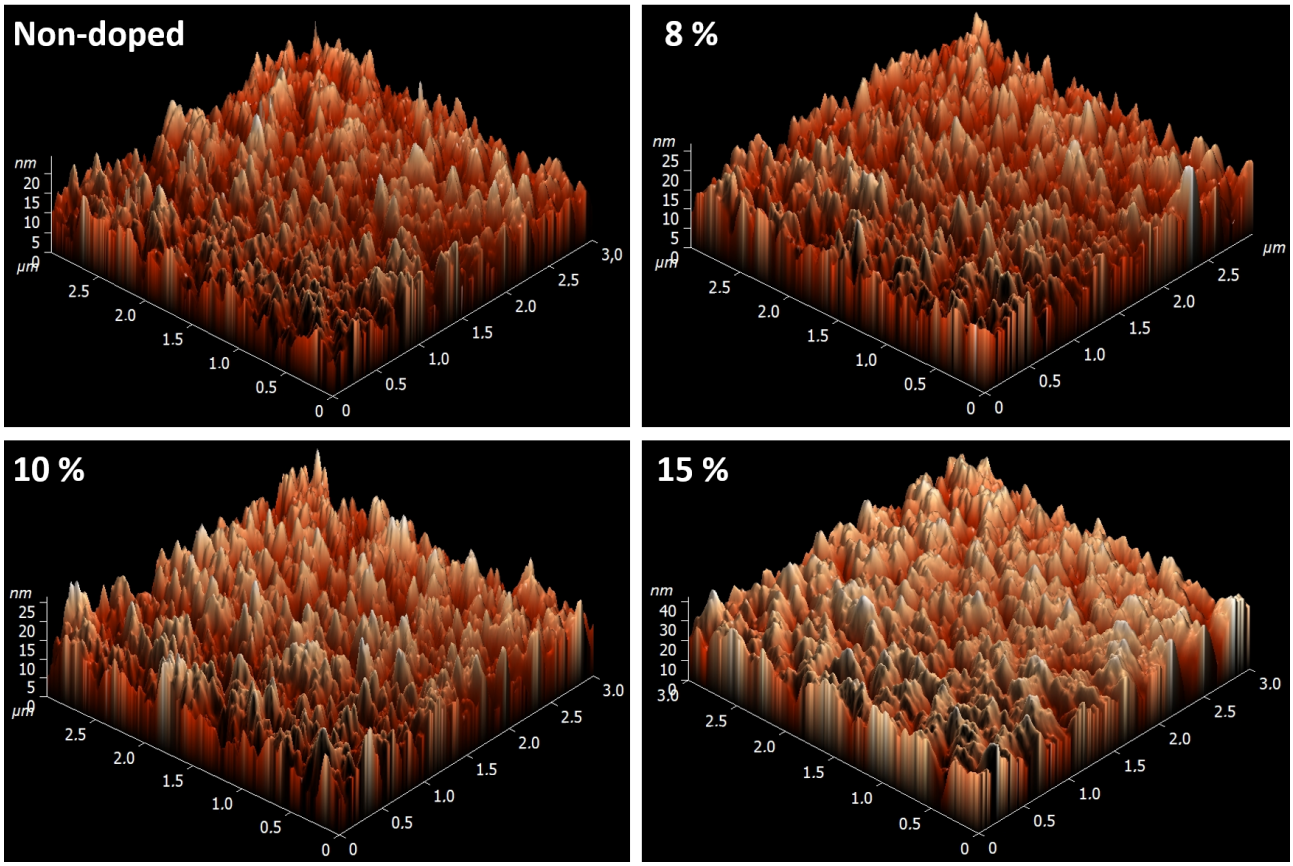

Figure 2. Representative 3D AFM images of PEDOT:PSS films (a) nondoped and doped with (b) 8 v/v.%, (c) 10 v/v.%, and (d) 15 v/v.% of mixed cosolvents of EG and MeOH.

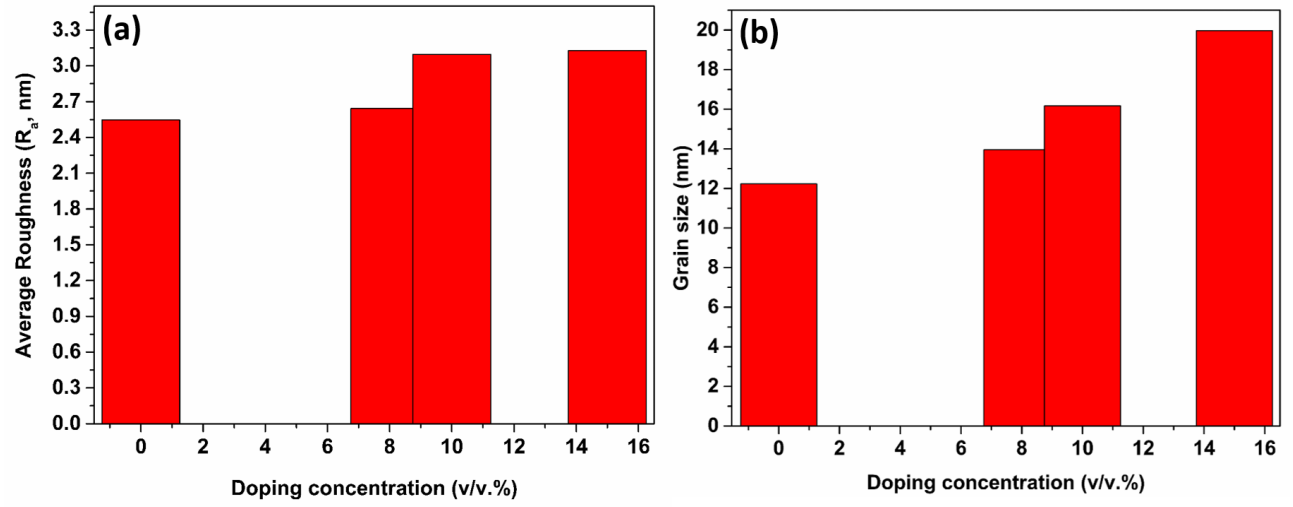

Figure 3. (a) Average surface roughness values and (b) grain size distribution obtained from the AFM images of PEDOT:PSS films.

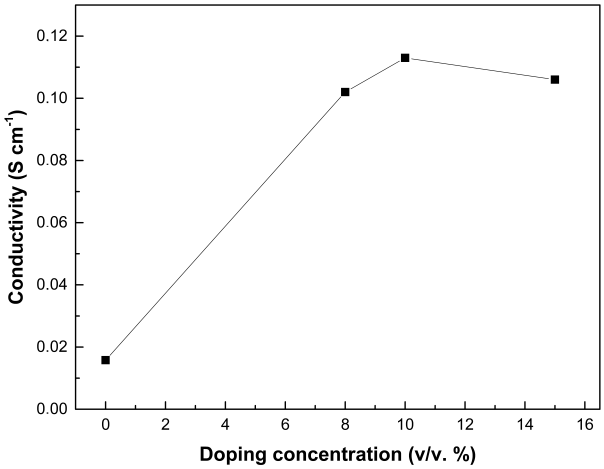

Figure 4. The conductivity of PEDOT:PSS films doped with 8, 10, 15 v/v.% of mixed cosolvents of EG and MeOH.

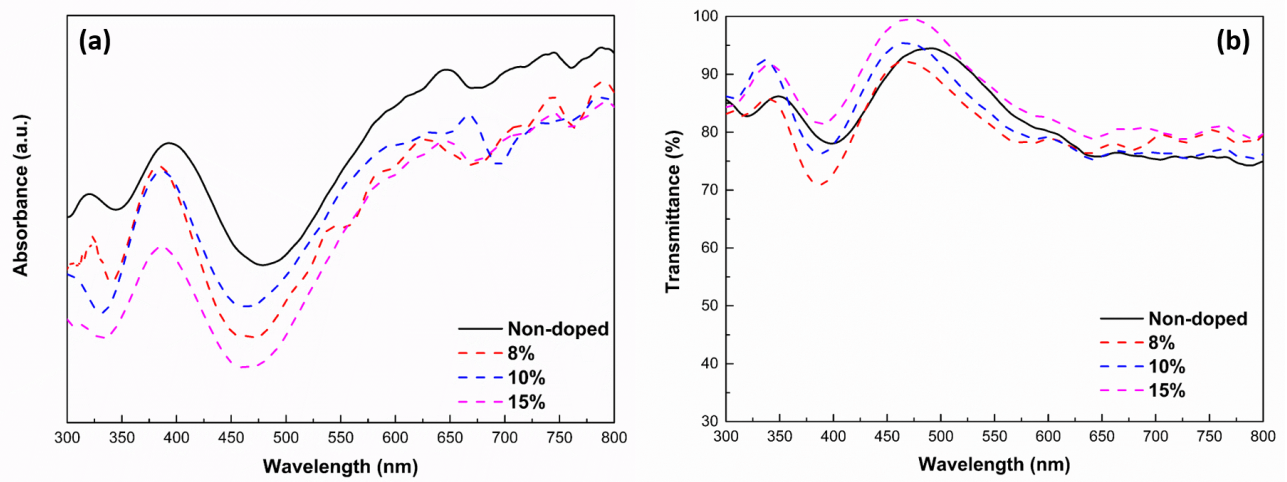

Figure 5. (a) UV-Vis absorption spectra and (b) optical transmission spectra of PEDOT:PSS films.

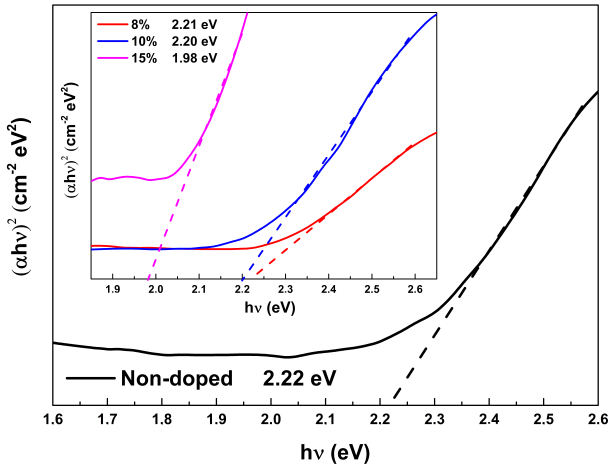

Figure 6. Optical band gap estimation from UV-Vis absorption spectra.

For the investigation of the mixed cosolvent addition to low conductive PEDOT:PSS on photovoltaic performance, PSCs were fabricated using PEDOT:PSS doped with various volumes of mixed cosolvent. From J-V measurements, short circuit current density (J_{sc}), open circuit voltage (V_{oc}), fill factor (FF), and PCE (?) were extracted under illumination conditions. The current density obtained at zero bias applied is J_{sc}, whereas the voltage at which no current flows is V_{oc} and theoretical maximum power that the cell can deliver is FF. The PCE is determined by dividing the maximum power point by the incident light irradiance (P_{in}), as given below (Eq. (1)):

$$\eta = \frac{J_{sc} V_{oc} FF}{P_{in}} \tag{1}$$

Figure 7a presents the current density–voltage (J-V) curves and the device performance parameters extracted from the J-V curves are given in Table 1. The control device produced with a nondoped PEDOT:PSS layer showed a PCE of 2.25% with a J_{sc} of 12.15 mA cm^{-2}, a V_{oc} of 0.455 V, and a FF of 40.7%. This PCE is comparable to results reported in the literature, which can be seen in Table 2 [31–35]. In comparison to the control device, all devices fabricated with a doped PEDOT:PSS layer yielded superior PCE thanks to enhanced V_{oc} and J_{sc} values, while the FF values were mostly unchanged. The device with 10 v/v.% mixed cosolvent-added PEDOT:PSS film achieved the highest PCE of 2.70% with a V_{oc} of 0.469 V and J_{sc} of 14.03 mA cm^{-2}. This significant improvement in photovoltaic performance could be explained by the improvement in the conductivity of PEDOT:PSS films doped with mixed cosolvent. Based on the results reported, the addition of mixed cosolvent to PEDOT:PSS solution as a low-cost, simple, and useful method that enhances the efficiency of P3HT:PCBM-based PSCs significantly.

Table 1. Summary of device parameters extracted from J-V curves presented in Figure 7.

Device	V_{oc} (V)	J_{sc} (mA/cm^2)	FF (%)	Efficiency (%)
Nondoped	0.455	12.146	40.68	2.248
8%	0.483	13.139	37.15	2.358
10%	0.469	14.026	41.02	2.698
15%	0.477	13.995	35.49	2.369

Table 2. The photovoltaic characteristics of PSCs reported in the literature similar to the control device fabricated in this study.

Device	V_{oc} (V)	J_{sc} (mA cm^{-2})	FF (%)	Efficiency (%)	Ref.
ITO/PEDOT:PSS/P3HT:PCBM/Al	0.62	3.87	55	1.31	[31]
ITO/PEDOT:PSS/P3HT:PCBM /LiF/Al	0.48	17.06	45	2.11	[32]
FTO/ZnO/P3HT:PCBM/Ag	0.52	7.01	50	1.91	[33]
ITO/PEDOT:PSS/P3HT:PCBM/Al	0.34	14.65	50	2.51	[34]
ITO/PEDOT:PSS/P3HT:PCBM/Ca/Al	1.19	5.61	38	2.54	[35]

The results present a simple and useful method to improve the photovoltaic parameters of inverted PSCs fabricated.

The shunt resistance (R_{sh}) and series resistance (R_s) of a solar cell could supply information about charge transport properties. There are many different methods to obtain R_{sh} and R_s. Roughly, R_s is the

slope of the J-V curve at zero voltage, while R_{sh} is the slope of the J-V curve at zero current. The obtained values from the J-V curves are shown in Table 3. The doped devices present improvements in R_s values from 27.4 Ω to 27.1 Ω. The R_s values of the devices with mixed cosolvent-added films slightly decreased with increasing ratio of doping until 10 v/v.%. Although the device still showed a high J_{sc} value at the doping of 15 v/v.%, the R_s value showed a small increase, which may be caused by increasing roughness. The variation in J_{sc} values corresponds to increasing conductivity after the addition of mixed cosolvent and the decreasing R_s values of the devices. The R_{sh} values were 27.5 Ω, 30.6 Ω, and 29.7 Ω for the devices fabricated with PEDOT:PSS films doped with 8, 10, and 15 v/v.% mixed cosolvent, respectively, which are higher than that of the control device (24.7 Ω). As the R_{sh} is mainly related to the leakage current because of the charge back recombination, the higher values of R_{sh} reflect lower leakage current [36]. Relatively low R_{sh} values are generally characterized in which the photocurrent is significantly smaller than for a commercial silicon cell [37]. It can be said that power losses occur in solar cells due to the alternate current path provided. This issue must be investigated before large-scale industrial applications.

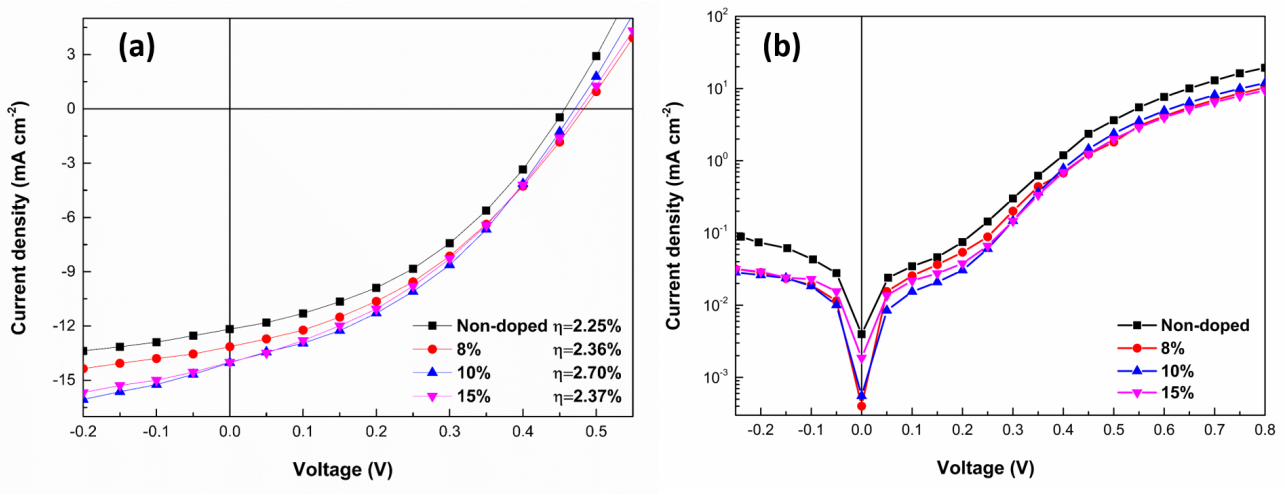

Figure 7. (a) The light and (b) the dark J-V curves of PSCs.

Table 3. The series (R_s), shunt resistances (R_{sh}), ideality factor (n), and dark saturation current density (J_o) extracted from dark and light J-V curves.

Device	R_s (Ohms)	R_{sh} (Ohms)	J_o	n
Nondoped	27.4	24.7	4.21 $\times 10^{-3}$	2.73
8%	27.4	27.5	1.76 $\times 10^{-3}$	2.64
10%	27.1	30.6	1.60 $\times 10^{-3}$	2.61
15%	29.7	29.7	1.74 $\times 10^{-3}$	2.63

For all devices, Figure 7b presents the J-V curves measured under dark conditions. The J-V characteristics under dark conditions can be identified by the Shockley–Read–Hall equation below:

$$J = J_o \left(exp \left(\frac{qV}{n\, k_B\, T} \right) - 1 \right), \tag{2}$$

where J and J_o are the current density and reverse saturation current density, respectively, and q is the elementary charge, n is the diode ideality factor, V is the applied voltage, k_B is the Boltzmann constant, and T is the absolute temperature. The n and J_o values calculated by using J-V measurements obtained under dark conditions are shown in Table 3. Strong doping ratio dependency for the n and J_o values was observed. Table 3 shows that the J_o values increase with the doping ratio. For the control device, the n value was calculated to be 2.73, whereas it was calculated to be 2.64, 2.61, and 2.63 for the devices fabricated with PEDOT:PSS films doped with 8, 10, and 15 v/v.% mixed cosolvent, respectively. Such a decrease indicates a reduction in the recombination rate [38]. These results obtained are consistent with the findings of the R_s and R_{sh} calculation. n values greater than unity indicate a deviation from the ideal diode, which could be attributed to nonuniformity of the absorber layer [39].

Figure 8 shows the EQE spectra of the control device and the champion cell prepared with PEDOT:PSS film at the doping of 10 v/v.%. An EQE of ~45% at 500–600 nm was calculated for the best solar cell, whereas EQE of ~40% was calculated for the control device. There is a significant enhancement decrease after mixed cosolvent doping. The results indicate that the doping process improves the solar spectral coverage and thus device performance.

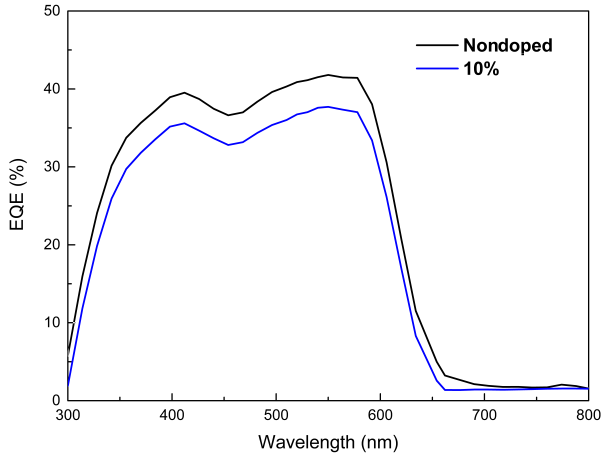

Figure 8. EQE of control and champion cell prepared with PEDOT:PSS film at the doping of 10 v/v.%.

Conclusions

In the present study, the effect of EG and MeOH mixture as a cosolvent additive on the morphological, electrical, optical, and energy bandgap properties of PEDOT:PSS thin films was demonstrated. It was found that the addition of EG and MeOH cosolvent mixture to PEDOT:PSS can enhance film conductivity. The doping of EG and MeOH cosolvent mixture into PEDOT:PSS enlarged grain size, indicating the aggregation of PEDOT-rich nanostructures on the surface, and improved conductivity. The film conductivity increased to 0.113 S cm^{-1} at the doping of 10 v/v.%. The doped PEDOT:PSS films were utilized to fabricate photovoltaic devices and their photovoltaic characteristics were characterized. The champion cell prepared with PEDOT:PSS film at the doping of 10 v/v.% (yielded a PCE of 2.7%) presented a 20% enhancement due to increased values of V_{oc} and J_{sc} and reduced recombination rate. This study provides a simple procedure to improve the morphological and electrical properties of low conductivity PEDOT:PSS. The characterization results would be useful to improve the PCE of PSCs.

References

[1] Liu Z, Zeng D, Gao X, Li P, Zhang Q et al. Non-fullerene polymer acceptors based on perylene diimides in all-polymer solar cells. Solar Energy Materials and Solar Cells 2019; 189: 103-117. doi: 10.1016/j.solmat.2018.09.024

[2] Li Y, Zou Y. Conjugated polymer photovoltaic materials with broad absorption band and high charge carrier mobility. Advanced Materials 2008; 20 (15): 2952-2958. doi: 10.1002/adma.200800606

[3] Kutsarov DI, Rašović I, Zachariadis A, Laskarakis A, Lebedeva MA et al. Achieving 6.7% efficiency in P3HT/Indene-C70 bisadduct solar cells through the control of vertical volume fraction distribution and optimized regio-isomer ratios. Advanced Electronic Materials 2016; 2 (12): 1600362. doi: 10.1002/aelm.201600362

[4] Huang S, Yu A, Wang Y, Tang Y, Shen S et al. Nickel oxide and polytetrafluoroethylene stacked structure as an interfacial layer for efficient polymer solar cells. Electrochimica Acta 2019; 299: 366-371. doi: 10.1016/j.electacta.2019.01.028

[5] Zhao W, Li S, Yao H, Zhang S, Zhang Y et al. Molecular optimization enables over 13% efficiency in organic solar cells. Journal of the American Chemical Society 2017; 139 (21): 7148-7151. doi: 10.1021/jacs.7b02677

[6] Zhang S, Qin Y, Zhu J, Hou J. Over 14% efficiency in polymer solar cells enabled by a chlorinated polymer donor. Advanced Materials 2018; 30 (20): 1800868. doi: 10.1002/adma.201800868

[7] Abdulrazzaq OA, Saini V, Bourdo S, Dervishi E, Biris AS. Organic solar cells: a review of materials, limitations, and possibilities for improvement. Particulate Science and Technology 2013; 31 (5): 427-442. doi: 10.1080/02726351.2013.769470

[8] Lu L, Luo Z, Xu T, Yu L. Cooperative plasmonic effect of Ag and Au nanoparticles on enhancing performance of polymer solar cells. Nano Letters 2013; 13 (1): 59-64. doi: 10.1021/nl3034398

[9] Huang S, Wang Y, Shen S, Tang Y, Yu A. Enhancing the performance of polymer solar cells using solution-processed copper doped nickel oxide nanoparticles as hole transport layer. Journal of Colloid and Interface Science 2019; 535: 308-317. doi: 10.1016/j.jcis.2018.10.013

[10] Lee JK, Ma WL, Brabec CJ, Yuen J, Moon JS et al. Processing additives for improved efficiency from bulk heterojunction solar cells. Journal of the American Chemical Society 2008; 130 (11): 3619-3623. doi: 10.1021/ja710079w

[11] Feng W, Song C, Hu X, Liu S, Yi R et al. Highly efficient charge collection in bulk-heterojunction organic solar cells by anomalous hole transfer and improved interfacial contact. ACS Applied Materials & Interfaces 2018; 10 (34): 28256-28261. doi: 10.1021/acsami.8b08390

[12] Chen Y, Kang KS, Han KJ, Yoo KH, Kim J. Enhanced optical and electrical properties of PEDOT: PSS films by the addition of MWCNT-sorbitol. Synthetic Metals 2009; 159 (17): 1701-1704. doi: 10.1016/j.synthmet.2009.05.009

[13] Yıldız DE, Karakuş M, Toppare L, Cirpan A. Leakage current by Frenkel–Poole emission on benzotriazole and benzothiadiazole based organic devices. Materials Science in Semiconductor Processing 2014; 28: 84-88. doi: 10.1016/j.mssp.2014.06.038

[14] Apaydın HA, Yıldız DE, Cirpan A, Toppare L. Optimizing the organic solar cell efficiency: role of the active layer thickness. Solar Energy Materials and Solar Cells 2013; 113: 100-105. doi: 10.1016/j.solmat.2013.02.003

[15] Shibata M, Sakai Y, Yokoyama D. Advantages and disadvantages of vacuum-deposited and spin-coated amorphous organic semiconductor films for organic light-emitting diodes. Journal of Materials Chemistry C 2015; 3: 11178-11191. doi: 10.1039/c5tc01911g

[16] Sivakumar G, Pratyusha T, Gupta D, Shen W. Doping of hole transport layer PEDOT: PSS with pentacene for PCDTBT: PCBM based organic solar cells. Materials Today: Proceedings 2017; 4 (7): 6814-6819. doi: 10.1016/j.matpr.2017.07.008

[17] Zhao Z, Wu Q, Xia F, Chen X, Liu Y et al. Improving the conductivity of PEDOT:PSS hole transport layer in polymer solar cells via copper(II) bromide salt doping. ACS Applied Materials & Interfaces 2015; 7 (3): 1439-1448. doi: 10.1021/am505387q

[18] Yan F, Parrott EPJ, Ung BSY, Pickwell-MacPherson E. Solvent doping of PEDOT/PSS: effect on terahertz optoelectronic properties and utilization in terahertz devices. The Journal of Physical Chemistry C 2015; 119 (12): 6813-6818. doi: 10.1021/acs.jpcc.5b00465

[19] Yamashita M, Otani C, Shimizu M, Okuzaki H. Effect of solvent on carrier transport in poly(3,4-ethylenedioxythiophene)/poly(4-styrenesulfonate) studied by terahertz and infrared-ultraviolet spectroscopy. Applied Physics Letters 2011; 99 (14): 143307. doi: 10.1063/1.3647574

[20] Vosgueritchian M, Lipomi DJ, Bao Z. Highly conductive and transparent PEDOT:PSS films with a fluorosurfactant for stretchable and flexible transparent electrodes. Advanced Functional Materials 2012; 22 (2): 421-428. doi: 10.1002/adfm.201101775

[21] Sun K, Xia Y, Ouyang J. Improvement in the photovoltaic efficiency of polymer solar cells by treating the poly(3,4-ethylenedioxythiophene):poly(styrenesulfonate) buffer layer with co-solvents of hydrophilic organic solvents and hydrophobic 1,2-dichlorobenzene. Solar Energy Materials and Solar Cells 2012; 97: 89-96. doi: 10.1016/j.solmat.2011.09.039

[22] Itoh K, Kato Y, Honma Y, Masunaga H, Fujiwara A et al. Structural alternation correlated to the conductivity enhancement of PEDOT:PSS films by secondary doping. The Journal of Physical Chemistry C 2019; 123 (22): 13467-13471. doi: 10.1021/acs.jpcc.9b02475

[23] Thomas JP, Leung KT. Mixed co-solvent engineering of PEDOT:PSS to enhance its conductivity and hybrid solar cell properties. Journal of Materials Chemistry A 2016; 4 (44): 17537-17542. doi: 10.1039/C6TA07410C

[24] Peng B, Guo X, Cui C, Zou Y, Pan C et al. Performance improvement of polymer solar cells by using a solvent-treated poly(3,4-ethylenedioxythiophene):poly(styrenesulfonate) buffer layer. Applied Physics Letters 2011; 98 (24): 243308. doi: 10.1063/1.3600665

[25] Zhao Y, Xie Z, Qu Y, Geng Y, Wang L. Solvent-vapor treatment induced performance enhancement of poly(3-hexylthiophene):methanofullerene bulk-heterojunction photovoltaic cells. Applied Physics Letters 2007; 90 (4): 043504. doi: 10.1063/1.2434173

[26] Alemu D, Wei HY, Ho KC, Chu CW. Highly conductive PEDOT:PSS electrode by simple film treatment with methanol for ITO-free polymer solar cells. Energy & Environmental Science 2012; 5 (11): 9662-9671. doi: 10.1039/C2EE22595F

[27] Hu Z, Zhang J, Hao Z, Zhao Y. Influence of doped PEDOT:PSS on the performance of polymer solar cells. Solar Energy Materials and Solar Cells 2011; 95 (10): 2763-2767. doi:10.1016/j.solmat.2011.04.040

[28] Alam KM, Kar P, Thakur UK, Kisslinger R, Mahdi N et al. Remarkable self-organization and unusual conductivity behavior in cellulose nanocrystal-PEDOT: PSS nanocomposites. Journal of Materials Science: Materials in Electronics 2019; 30 (2): 1390-1399. doi: 10.1007/s10854-018-0409-y

[29] Gravalidis C, Laskarakis A, Logothetidis S. Fine tuning of PEDOT electronic properties using solvents. The European Physical Journal Applied Physics 2009; 46 (1): 12505. doi: 10.1051/epjap/2009030

[30] Xiang HJ, Huang B, Kan E, Wei SH, Gong XG. Towards direct-gap silicon phases by the inverse band structure design approach. Physical Review Letters 2013; 110: 118702. doi: 10.1103/PhysRevLett.110.118702

[31] Kadem B, Kaya EN, Hassan A, Durmuş M, Basova T. Composite materials of P3HT:PCBM with pyrene substituted zinc(II) phthalocyanines: characterisation and application in organic solar cells. Solar Energy 2019; 189: 1-7. doi: 10.1016/j.solener.2019.07.038

[32] Kaçuş H, Aydoğan Ş, Biber M, Metin Ö, Sevim M. The power conversion efficiency optimization of the solar cells by doping of (Au:Ag) nanoparticles into P3HT:PCBM active layer prepared with chlorobenzene and chloroform solvents. Materials Research Express 2019; 6: 095104. doi: 10.1088/2053-1591/ab309a

[33] Lim EL, Yap CC, Jumali MHJ, Khairulaman FL. Solution-dispersed copper iodide anode buffer layer gives P3HT:PCBM-based organic solar cells an efficiency boost. Journal of Materials Science: Materials in Electronics 2019; 30: 2726-2731. doi: 10.1007/s10854-018-0548-1

[34] KırmacıE, Dinçalp H, Murat Saltan G, Kıran M, Zafer C. Small biomolecule dopant retinals: electron blocking layer in P3HT:PCBM type organic solar cells. Synthetic Metals 2018; 236: 8-18. doi: 10.1016/j.synthmet.2017.11.012

[35] Aïssa B, Nedil M, Kroeger J, Ali A, Isaifan RJ et al. Graphene nanoplatelet doping of P3HT:PCBM photoactive layer of bulk heterojunction organic solar cells for enhancing performance. Nanotechnology 2018; 29: 105405. doi: 10.1088/1361-6528/aaa62d

[36] Caliò L, Kazim S, Salado M, Zimmermann I, Khaja M et al. Design of cyclopentadithiophene-based small organic molecules as hole selective layers for perovskite solar cells. Sustainable Energy & Fuels 2018; 2 (10): 2179-2186. doi: 10.1039/C8SE00119G

[37] Bouzidi K, Chegaar M, Bouhemadou A. Solar cells parameters evaluation considering the series and shunt resistance. Solar Energy Materials and Solar Cells 2007; 91 (18): 1647-1651. doi: 10.1016/j.solmat.2007.05.019

[38] Kadem B, Hassan A, Cranton W. Efficient P3HT:PCBM bulk heterojunction organic solar cells; effect of post deposition thermal treatment. Journal of Materials Science: Materials in Electronics 2016; 27 (7): 7038-7048. doi: 10.1007/s10854-016-4661-8

[39] Yıldız DE, Apaydın DH, Kaya E, Altindal S, Cirpan A. The main electrical and interfacial properties of benzotriazole and fluorene based organic devices. Journal of Macromolecular Science, Part A: Pure and Applied Chemistry 2013; 50: 168-174. doi: 10.1080/10601325.2013.741864